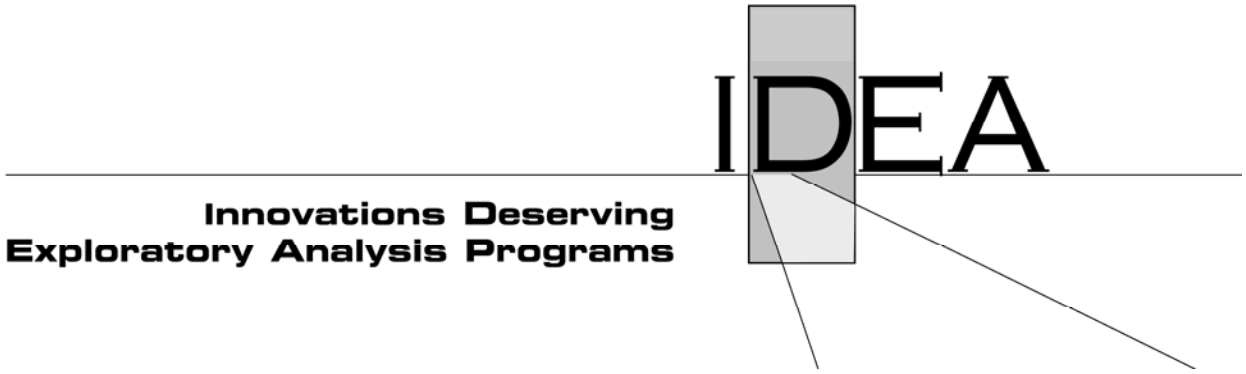

Highway IDEA Program

Dual Core FTDM Fiber Optic WIM System

Final Report for Highway IDEA Project 42

Prepared by:
Ramesh B. Malla and Norman W. Garrick, University of Connecticut

October 2000

TRANSPORTATION RESEARCH BOARD
OF THE NATIONAL ACADEMIES

INNOVATIONS DESERVING EXPLORATORY ANALYSIS (IDEA) PROGRAMS
MANAGED BY THE TRANSPORTATION RESEARCH BOARD (TRB)

This NCHRP-IDEA investigation was completed as part of the National Cooperative Highway Research Program (NCHRP). The NCHRP-IDEA program is one of the four IDEA programs managed by the Transportation Research Board (TRB) to foster innovations in highway and intermodal surface transportation systems. The other three IDEA program areas are Transit-IDEA, which focuses on products and results for transit practice, in support of the Transit Cooperative Research Program (TCRP), Safety-IDEA, which focuses on motor carrier safety practice, in support of the Federal Motor Carrier Safety Administration and Federal Railroad Administration, and High Speed Rail-IDEA (HSR), which focuses on products and results for high speed rail practice, in support of the Federal Railroad Administration. The four IDEA program areas are integrated to promote the development and testing of nontraditional and innovative concepts, methods, and technologies for surface transportation systems.

For information on the IDEA Program contact IDEA Program, Transportation Research Board, 500 5th Street, N.W., Washington, D.C. 20001 (phone: 202/334-1461, fax: 202/334-3471, http://www.nationalacademies.org/trb/idea)

ACKNOWLEDGMENTS

The study has been financially supported, in part, by the National Academy of Sciences, Washington D.C. under the National Cooperative Highway Research Program (NCHRP)-Innovations Deserving Exploratory Analysis (IDEA) Type 1 (Concept Feasibility) investigation (NCHRP Project - 42). The support is gratefully acknowledged. The work reported herein was performed at the University of Connecticut, Storrs, CT. Dr. Ramesh B. Malla, Associate Professor of Department of Civil & Environmental Engineering was the principal investigator for the research project. Support from Metrilight, Inc. , Southbridge, MA, for providing the special optical fiber is greatly appreciated. The research team also acknowledge the financial and other support received from the University of Connecticut, in particular the Department of Civil and Environmental Engineering, School of Engineering, Photonics Research Center, and the Institute of Materials Science.

Several individuals assisted in the project. Their contributions are duly acknowledged. First of all, Dr. Marcos Kleinerman, CEO of the industrial affiliate MetriLight, Incorporated provided invaluable technical consulting and advice on the patented special dual-core optical fiber used in this project. Dr. Eric Donkor, Associate Professor of Electrical and Computer Engineering of the University of Connecticut assisted by giving useful comments and advice time to time on general optical fiber concepts and instrumentation. Sincere thanks are due to Mr. Amlan Sen, Ms. Puneit Dua and Mr. Yuyang Lin who worked on this project during their graduate work and carried out most of the experimental investigations.

Last but not least useful comments from the Project Advisory panel members is gratefully acknowledged. The members of the Project Advisory panel were: Dr. Farhad Ansari (University of Illinois at Chicago, previously at the New Jersey Institute of Technology), Dr. Robert Gubala (Member, NCHRP-IDEA Project Committee; previously at the Connecticut Department of Transportation), Ms. Amy Jackson-Grove (FHWA Regional Office, Connecticut), Ms. Ann Marie McDonnell (Connecticut Department of Transportation), and Dr. William Morey (3M at Austin, TX; previously at 3M Bragg Grating Technology, Connecticut). Special thanks to the advisory panel member Dr. Robert Gubala, who also served as the local mentor for the project and provided valuable feedback and constructive comments. Sincere thanks are due to Dr. Inam Jawed, NCHRP-IDEA Program Manager for his useful comments, advice and help throughout the project duration. Finally, special thanks to Mr. Jagdeesh Gopal for helping to prepare this report.

TABLE OF CONTENTS

Title Page	i
Acknowledgments	ii
Table of Contents	iii
Chapter 1.0 Executive Summary	1
Chapter 2.0 Project Description	3
2.1 Introduction	3
2.2 IDEA Product	4
2.3 Concept and Innovation	4
2.3.1 Description of the Fiber	4
2.3.2 Fiber Geometry and Dimensions	6
2.4 Investigation	6
2.4.1 Optical Characteristics of Fiber	6
2.4.1.1 Experimental Set-Up	7
2.4.1.2 The Bending Experiment	7
2.4.2 Prototype Development	9
2.4.2.1 Proposed WIM Device	10
2.4.2.2 Design of Top Curved Plate	11
2.4.2.3 Design of Springs	13
2.4.2.4 Design of Pins	13
2.4.2.5 Overall Design Details	14
2.4.3 Prototype Testing	15
2.4.3.1 Test under Loading Machine	15
2.4.3.2 Test Under Vehicle Wheel	15
2.4.4 Test Results	16
2.4.4.1 Results from SATEC Machine	17
2.4.4.2 Analysis of SATEC Test Results	18
2.4.4.3 Concept of Bent Length of Fiber	19
2.4.4.4 Car Test Data	21
2.4.5 Computer Data Acquisition	22
2.5 Plans for Implementation	24
Chapter 3.0 Conclusions And Recommendations	25
3.1 Conclusions	25
3.2 Recommendations for Future Work	25
Glossary and References	26

CHAPTER 1.0
EXECUTIVE SUMMARY

Highway deterioration accelerates exponentially as truck weight increases. Accurate data on vehicle weights are essential for the design and management of highway pavements. Currently, we do not have comprehensive data on the weight distribution of vehicles using our highways. Reliable, inexpensive and easy-to-use Weigh-in-Motion (WIM) system would help to correct this problem resulting in improved highway design procedures. Each year over $7 billion is spent on highway construction, rehabilitation and maintenance: improved WIM technology will help to save a significant fraction of this direct cost. The cost of traffic data collection process is also expected to decrease with the development of this product. This report presents the work accomplished under the National Cooperative Highway Research Program (NCHRP)-Innovations Deserving Exploratory Analysis (IDEA) Type 1 (Concept Feasibility) investigation on the Dual Core Forward Time Division Multiplexing (FTDM) Fiber Optic WIM System (NCHRP Project - 42).

The final product from our work will be a fiber optic sensor system for weighing and counting highway vehicles. This weigh-in-motion (WIM) system will be used on roads that are functioning under normal conditions and will cause no disruption to traffic. The technological break through behind this WIM sensor is a unique dual core optical fiber which is radically different from most fibers that are currently being used in civil engineering and other sensing applications. We anticipate that our WIM will be simpler to install and operate and will be more accurate than comparable devices.

The anticipated enhanced capabilities of this system directly results from the inherent advantages of our dual core fiber compared to the conventional sensor fiber technology. Our fiber has two concentric light guiding regions of different effective optical path length: this design enables us to measure magnitude as well as positions of forces that are applied at multiple locations along a single fiber and using a single light source and photodetector. We anticipate that this device will be configured to give not only vehicle weight and volume but also speed, inter-axle distance and lateral vehicle location.

We designed and fabricated a prototype WIM system and have tested the system both with loading machines and with an actual vehicle. As a part of this process, we characterized and calibrated the optical fibers used in the system. In the vehicle test, the prototype WIM was installed between wooden tracks that were used to simulate a pavement. The vehicle (a passenger car) was then driven over the system and the optical signal was recorded for various locations of the car wheel over the prototype WIM device (Figures 1 and 2).

The test results on the behavior of the available batch of the special optical fiber revealed that the fiber had some deviation from the theoretically expected behavior. Within this limitation, the laboratory test results of the prototype WIM proved to be very promising. The load test showed a very good relationship between the magnitude of the applied load and the changes in the optical signal. Furthermore, the changes in the optical signal during testing with the car were quite similar to that obtained for the load machines. Figure 1 shows the car wheel testing in progress. Figure 2 shows the time delay of the output light pulses traveling through the fiber before and after the vehicle wheel load. This time delay allows to pinpoint the location of load application to a fair degree of accuracy. The intensity change in the signal before and after the load gives a good measure of the magnitude of the wheel load. Based on these results we believe that our prototype shows great potential for accurately determining the magnitude and location of vehicular loads. Toward the end of the project duration, we developed an automated computer system to acquire and analyze the data from the prototype WIM sensor device.

The test results have given us the information needed to improve the performance of the special fiber, configuration of the WIM system and in general to optimize our prototype in terms of size and performance. We intend to design and build a second-generation prototype and to conduct additional tests to fully characterize its performance. In addition, we are working on developing a dedicated optical system that will be rugged enough for field-testing.

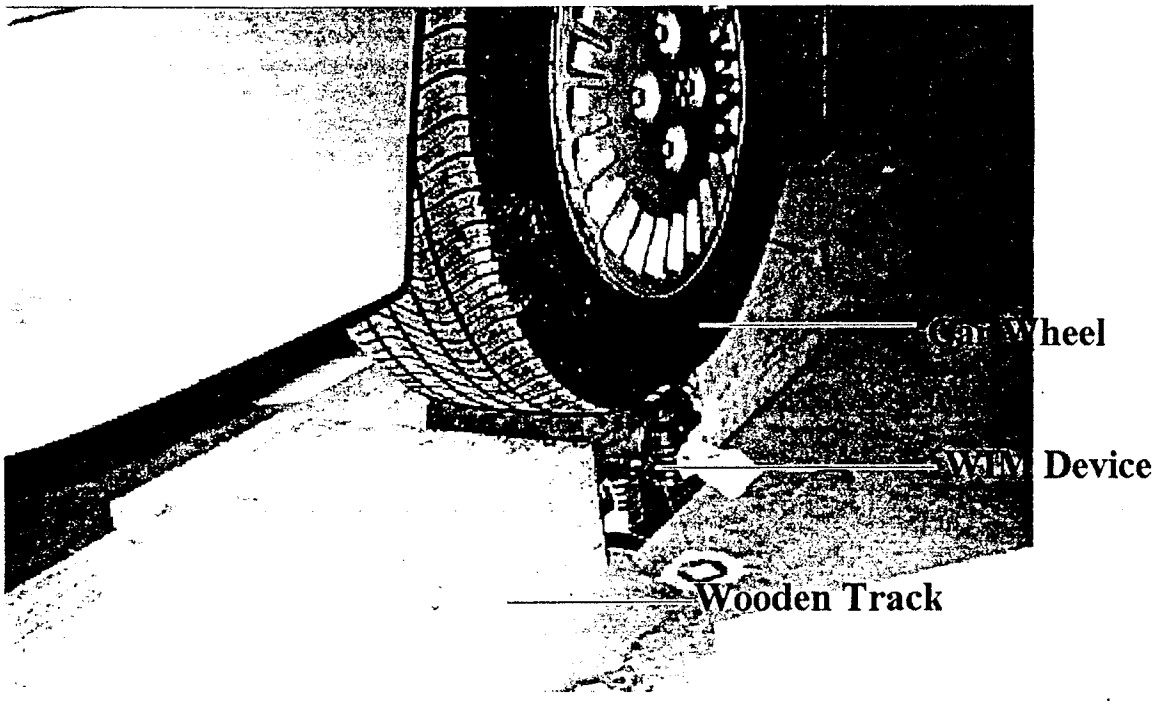

FIGURE 1 Car Wheel testing in Progress

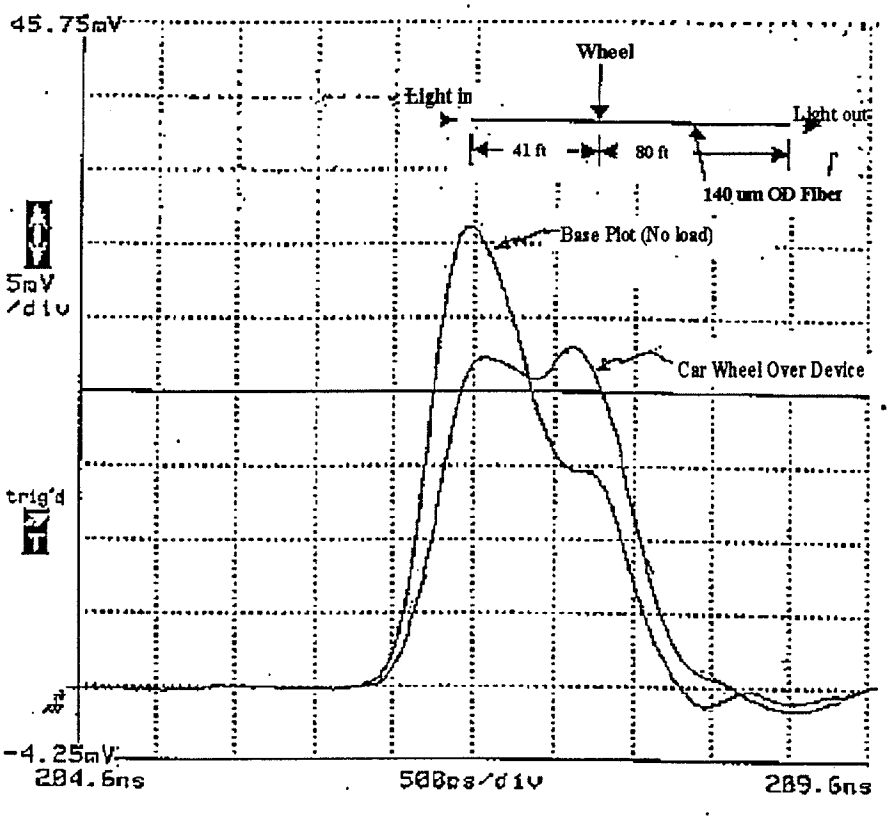

FIGURE 2 Oscilloscope Traces from Car Test

CHAPTER 2.0
PROJECT DESCRIPTION

This section describes the complete project work. This includes evaluation of the special optical fiber performance, development of Weigh in Motion (WIM) prototype device, testing protocols and results.

2.1 INTRODUCTION

Accurate measurement of static axle or wheel load has long been a major objective of highway engineers around the world. The static weight of a vehicle is used to provide a basis for pavement analysis and design *(1)*. Traditionally these weights have been collected by pulling the vehicles off the roadway and weighing them at weigh stations while the vehicles are at rest.

The advantages of weighing vehicles while they are in motion rather than at rest are numerous *(2)*. Conventional vehicle weighing systems are typically large, permanently installed and require the vehicle to remain stationary during the weighing process. In some cases where portable scales are used, the measurement process is further complicated by the enormous size and complexity of the vehicles being weighed. In these instances, dozens of portable static load cells are required for each measurement. The size, the weight of these load cells and the time required to accurately measure the weight is excessive *(3)*. Also, conventional weighing methods are only applicable on roads carrying low truck volumes or in instances in which only a small sample of the vehicle population is measured. On heavily trafficked roads, the weighing process can be extremely dangerous because of the long queue of trucks that tends to back-up from the weigh station on to the freeway.

The concept of Weigh-In-Motion (WIM) was introduced about forty years ago because of the problems associated with conventional weighing methods. Weigh-In-Motion is the process by which the weights of vehicles are measured while the vehicles are in motion. In theory, vehicles no longer have to get off the freeway to be weighed and so the weighing process is much faster. The corresponding static weights of the vehicles can then be estimated from the WIM measurements.

The first system of weighing highway vehicles in motion was reported by Norman and Hopkins *(4)*. Since then research on developing an ideal weigh-in-motion has been performed by many researchers worldwide *(5 - 14)*. A number of different WIM systems for weighing highway vehicles have been developed during the past four decades. These systems have been used generally by public agencies for collecting statistical traffic data, for aiding traffic law enforcement and in some cases for actual enforcement. WIM data has also been found to be very useful for a wide range of transportation and highway related planning and decision making objectives *(15 - 18)*. The three WIM systems that are used most often are capacitive pad transducers *(19)*, piezo-electric cables *(20)* and load cell systems *(19)*. However, these WIM systems give inconsistent readings due to temperature fluctuation, vehicle speed variations, and environmental factors. They are also relatively complex in design and require complex data acquisition and analysis systems. An extensive evaluation of the advantages and disadvantages of these systems have been reported *(21-23)*.

Sensing systems based on fiber optics have found increasing applications in telecommunications, electrical devices, aerospace structures and in the medical field. Optical fibers have several positive attributes, including (a) small diameter, (b) light weight, (c) immunity to electromagnetic interference, (d) utility in hostile environments (such as in presence of high voltage and high temperature), (e) high sensitivity and (f) ability to transmit data as well as serving as a sensor *(25)*. Due to these positive attributes of optical fibers, recently effort has been directed towards developing WIM systems using fiber optics *(3, 24-26)*.

One of the sensing systems using optical fibers is based on the optical time domain reflectometry (OTDR) technique in which the magnitude of the mechanical forces is measured by the decrease they cause in the intensity of the Rayleigh-backscatter from interrogating light pulses. A serious shortcoming of this technique is that it ejects light from the fiber on bending and, hence, provides an estimate of the load by comparing two very weak and noisy Rayleigh-back scattered signals.

Optical fiber techniques proposed for WIM systems, include those based on light polarization, interferometry *(24)* and on the modulation of light intensity through an optical fiber having a single core*(3, 27)*. Interferometric techniques are complicated and require a different interferometer for each fixed sensing point. On the other hand, the main disadvantage

of the polarization technique is that a polarization change at any point along the fiber affects the polarization state of the fiber at other sensing points. The technique based on light transmission along a single core has the disadvantage that it is not able to determine locations of forces applied at different points of the fiber.

In this project we investigated a new fiber technique for direct measurement of the weight of vehicles in motion. This technique is based on a special patented Dual Core Forward Time Division Multiplexing (FTDM) fiber. Under this system, the magnitude and the position of the load can be measured simultaneously. The system also has the advantage of providing an output signal with high intensity, thus allowing easier detection and measurement. In this project, we first tested the mechanical and optical properties of the fiber. We then designed our WIM load transmitting device. Finally, we tested this load transmitting device under both loading machine and passenger car wheel loads.

2.2 IDEA PRODUCT

The product from our work will be a sensor for weighing and counting highway vehicles. This weigh-in-motion (WIM) system will be used on roads that are functioning under normal conditions and will cause no disruption to traffic. The technological break through behind this WIM sensor is a unique dual core optical fiber which is radically different from most fibers that are currently being used in civil engineering and other sensing applications. We anticipate that our WIM will be simpler to install and operate and will be more accurate than comparable devices.

2.3 CONCEPT AND INNOVATION

The proposed Weigh-in-Motion (WIM) device is based on using a new optical fiber as the load sensor *(28)*. This fiber optic is the product of a new wave of fiber optic technology. The fiber used in this project has two light guiding regions of different effective optical lengths. Light injected into the fiber will take different times to travel through these two regions. This unique design allows for measurement of forces (magnitude and location) at multiple points along a single, continuous fiber and requires the use of just a single interrogating light source and a single photo detector. In this section we will discuss the operating principle of the fiber, the equipment set-up for using the fiber and the optical tests performed on the fiber.

2.3.1 Description of the Fiber

Figure 3 shows schematic diagrams of the cross section and the refractive profile of the fiber. The fiber comprises of the following four regions; i) a small single mode central (inner) core light guiding region (A), ii) a cladding (B) around the single mode core, iii) a second multimode graded index light-guiding region (C) around cladding, B, and finally iv) an outer cladding (D). The refractive index, n_1, of region A, is higher than the refractive index, n_2 of the cladding region B. Region C (outer core) has a graded near parabolic refractive index, n_3, which is substantially higher than that of the inner core (region A). The outer cladding D has a refractive index, n_4, which is substantially lower than that of the inner cladding (region B).

When a train of light pulses of the order of a nanosecond or shorter duration is launched into the fiber core, at the fiber launch end, a lateral mechanical force applied at any point along the fiber will deflect a fraction of the intensity of each of these interrogating light pulses from the inner core, to the graded index region, C (outer core). Because of the arrangement (Figure. 3) of the refractive index profile of the fiber, the deflected light is captured within this graded index core, C, and transmitted to the other end of the fiber. Since the refractive index of the outer light guiding region, C, is substantially greater than the refractive index of the inner light guiding region, A, the light pulses carried by the outer core will arrive at the fiber output end Δt seconds after the arrival of the undeflected light pulses transmitted by the central inner core (Figure 4). This time interval is proportional to the distance measured from the output end along the fiber of the location at which the force is applied. This relation is given by the following equation:

$$\Delta t = (z/c)(n_3 - n_1) \qquad (1)$$

Where z is the distance from the output end of the fiber to the location where the force is applied and c is the speed of light in free space.

Since some of the light escapes into the outer core, there is a loss in the intensity of the light traveling in the inner core. The magnitude of the force can be determined from the relative intensities of these two light signals traveling along inner and outer cores. Apart from measuring the load and the location of the load, it is envisioned that our fiber can be used to determine the vehicular speed, number of axles, inter-axle distance, weight-distribution on each wheel and the traffic volume.

The separation of the inner and outer core signals in time is called "Forward Time Division Multiplexing (FTDM)". The deflected signal (light traveling in the outer core) in the FTDM fiber is several orders of magnitude stronger than other scattered light signal like the Rayleigh-backscattered light signal. In the Rayleigh-backscattered light signal, a small fraction of the input light is scattered from the impurities in the fiber and is sent back to the source end. When light is scattered out of the core due to mechanical disturbances, less light is present in the fiber initially and hence still less light will be scattered back. Therefore, in the Rayleigh-backscattering method we are basically comparing two very weak signals for our measurement and, as such, it is not an accurate method of measurement.

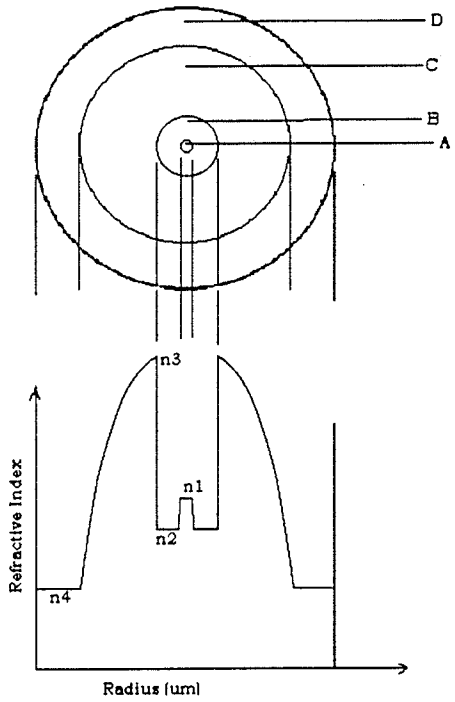

FIGURE 3 Dual Core FTDM Fiber (a) Cross-Section, (b) Representative Refractive Index Profile

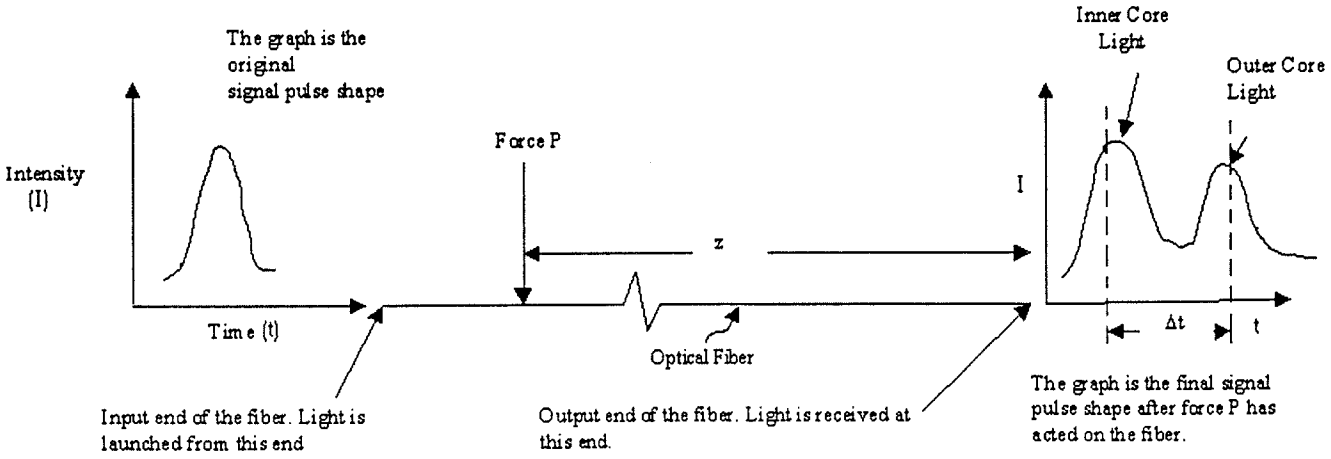

FIGURE 4 Input and Output Light Signals Through the Fiber

2.3.2 Fiber Geometry and Dimensions

For our experiments, we had fibers manufactured with two outer diameters, one with 125 μm diameter and the other with 140 μm diameter. We photographed the cross-section of the fibers using a NIKON transmission mode optical microscope having a magnification of 504. For 125 μm diameter fiber (Fiber 1) the cross section photograph is shown in Figure 5. In this figure, we can see all the four optical regions of the fiber. The fiber having diameter of 140 μm (Fiber 2) was used for most of our experiments. Fiber 2 was selected over Fiber 1 due to the fact that more light could be launched into the inner core of this fiber as the core diameter is a bit larger. Hence the output signal from this fiber (Fiber 2) is expected to be stronger and could be more conveniently recorded. Table 1 gives the dimensions of various regions of the fiber cross-section.

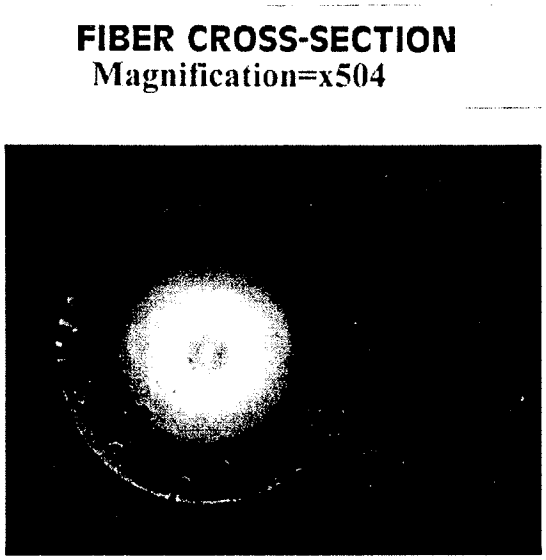

FIGURE 5 Cross Section of Optical Fiber

TABLE 1 Diameters of the Various Regions in the Fiber Cross Section

Region	Diameter (μm.): Fiber 1	Diameter (μm.): Fiber 2
Inner Core (A)	6	7
Inner Cladding (B)	18	18
Outer Core (C)	78	85
Outer Cladding (D)	125	140

2.4 INVESTIGATION

This section describes tests on the fiber and prototype WIM device and presents most significant results.

2.4.1 Optical Characteristics of Fiber

The optical characteristic of the fiber was assessed by bending the fiber by hand and measuring the output light signals. The purpose of these bending tests was to validate the theoretical principle of the fiber and to study the relationship

between the degree of bending and the optical output. This information is crucial in designing the mechanical system that is needed to transmit wheel load to the fiber.

2.4.1.1 Experimental Set-Up

The experimental set-up for the bending tests, which is shown in Figure 6, consisted of the following:

- A light source. (This consisted of a laser diode driven by a pulse generator.)
- The dual core FTDM optical fiber.
- The apparatus for receiving the light pulses and converting the light energy to electrical energy. (This consisted of the photo detector)
- The apparatus to display the output electrical signals. (This was the oscilloscope.)

In the laboratory experiment (Figure 6) the interrogating light pulses were obtained by modulating the laser diode with a pulse generator (Avtech Model no. AVM-2-C). The pulsed light beam from the laser diode was focused with a lens system onto the fiber so that most of the light entered the inner core. Fiber holders were used to firmly position the input end of the fiber.

At the output end of the fiber, a fiber holder similar to the one at its input end was placed to position the fiber. A second lens system was used to focus the light to a photo-detector. The photo-detector converted the light into electrical energy, which in turn is transmitted to the oscilloscope. In order to determine the most suitable combination of the laser diode and the photo-detector, various laser diodes in the wavelength range of 670-830 nm with output power in the range 5-30mW were tried with three different photo-detectors. One was a Silicon Avalanche Photo Detector (Newport Model No. 877APD). The second was an Ultrafast InGaAs Amplifier detector (Newport Model No. AD-300DC-FC), and the third was a 10 GHz ultra-fast photodetector (Hamamatsu Model ultrafast GaAs MSM photodetector G4176).

The electrical energy obtained from the photo-detector was very low when the Hamamatsu ultrafast GaAs MSM G4176 model photodetector was used. Therefore, a pre-amplifier connected with the photodetector by a Bias-T (Mini Circuits, Model 2FBT-6GW) was used to boost the current. This current is sent as input to the oscilloscope. The oscilloscopes used in different experiments for observing the output pulses were HP modular oscilloscope (Model No.54720D) and Tektronix 11801B oscilloscope.

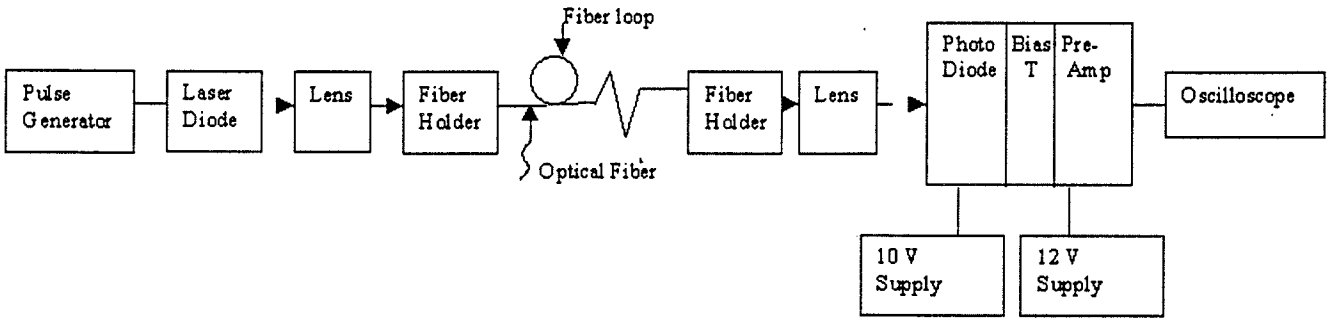

FIGURE 6 Optical Fiber Experimental/Test Set-Up

2.4.1.2 The Bending Experiment

This experiment was used to validate the behavior of the fiber with bending. The aim of the experiment was to quantify the changes in the output signal as a function of the bending radius. The fiber with 140 μm outer diameter was bent at a point into circular loops of different radii near the light input end of the fiber (Figure 6). The corresponding light output signals were observed using the HP 54720D oscilloscope. The total length of the fiber for these experiments was approximately 100 meters.

Figure 7 shows oscilloscope traces of the output signals from the fiber (with and without bending). Peak 1 is the light from the inner core while peak 3 corresponds to the light from the outer core that is leaked from the inner core to the

outer core at the bending location of the fiber. The possible cause for Peak 2 is explained below. Also as we see from the two oscilloscope traces (with and without bending), the magnitude of Peak 1 (inner core light) decreases due to the bending of the fiber and a new peak (Peak 3) appears.

The traces show that the theoretically expected behavior of the fiber is essentially correct as discussed in Sub-section 2.3.1. However, when there was no bending of the fiber, if all light were launched into the single mode inner core (region A, Figure 3) we should see only one peak (Peak 1) as the output signal. One such output peak would suggest that all the light stayed in the inner core throughout its journey through the fiber. But, in our experiment, we observed two peaks, (Peak 1 and Peak 2) instead of one peak even when there was no bending of the fiber.

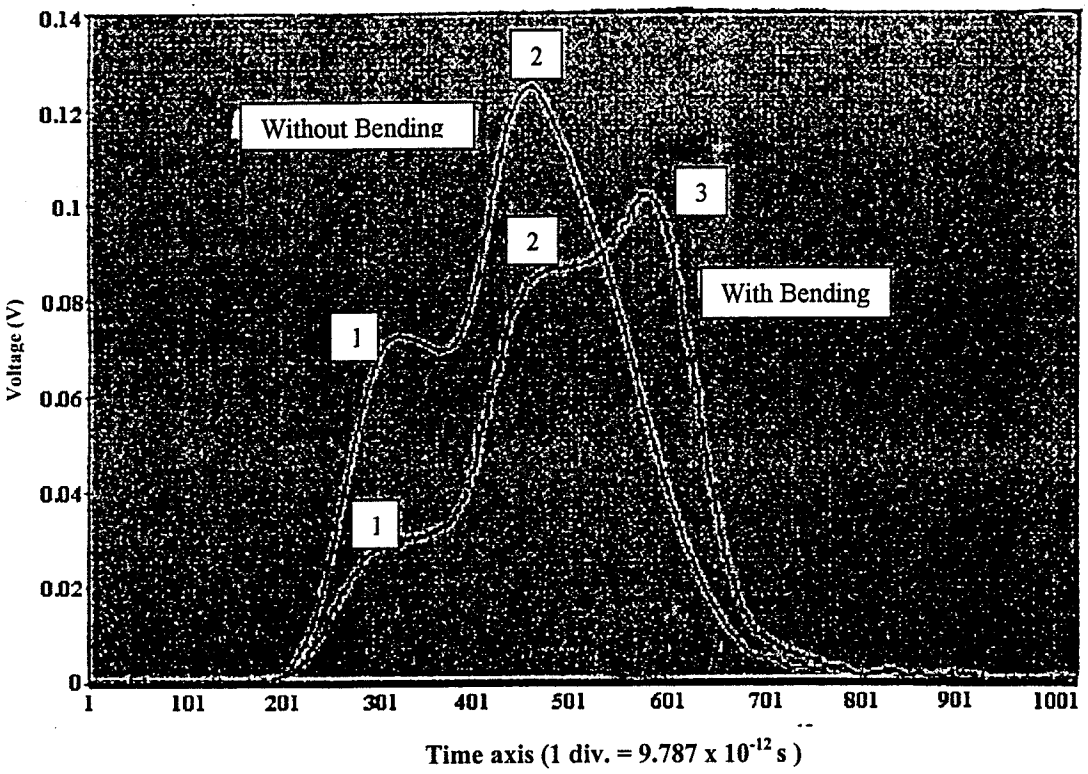

FIGURE 7 Oscilloscope Traces of 125 um Fiber for Bending and Without Bending Cases

There could be several possible explanations for this additional peak (Peak 2) in the light output signals. Some of them include

1. the possibility of a bend somewhere near the middle of the fiber.
2. a continuous leakage of light from the inner core to the outer core.
3. the possibility that the light could have been launched not only into the inner core, but also into the outer core at the input end of the fiber.
4. the possibility of mode mixing most of the light as it traveled through the graded index multimode region.
5. the possibility of the inner cladding (Region B, Figure.3) also guiding light along the fiber.
6. other.

Several experiments were conducted to try to isolate the cause of the extra peak. The multimode region experiments are discussed below.

An occurrence of a bend in the fiber could have resulted from the fact that the fiber was wound around a spool. Therefore, we unwound the fiber from the spool and laid it out straight. Even in this case, we did see the extra peak and therefore concluded that the peak could not have resulted from a bend in the middle of the fiber.

Continuous leakage of light could have occurred either from the fiber being wound in the spool or because of a manufacturing defect. By completely unwinding the fiber from the spool and repeating the test with the fiber placed

straight, we concluded that the winding of the fiber did not cause the additional peak. A continuous leakage of light throughout the fiber length would have caused a very wide output peak. Because we did not see such a signal, we ruled out the possibility of leakage of light from the inner to outer core throughout its length.

Another possible explanation for the extra light peak (Peak 2) to occur is that the light from the source was being directly launched not just into the inner core but also into the outer core of the fiber. It could be argued that if this was the case, then bending the fiber at the input end (as was the case in our experiment) would have caused the second and third peaks (Peaks 2 and 3) to coincide since we would then have two pulses (one from the light source directly and another from bending the fiber at about the same location) going through the same entire outer core fiber length. But this is not what we see in our output signal. Therefore, this reason could have been easily ruled out for causing the extra peak.

However, the outer core is a multimode region and light of several different modes than that which leaks out from the inner single mode core may travel through this region. Mode mixing may occur causing widening of the pulse width and affecting the time of travel through the region. Therefore, the output signal peak location and shape could be different from what we would have had if light of only a single mode traveled through the region.

If the inner cladding (Region B in Figure 3) guided light along the entire length of the fiber, Peak 1 corresponds to the light traveling through this region, Peak 2 corresponds to the inner core region and Peak 3 corresponds to the light through the outer core region. This could happen if the fiber is not manufactured correctly. However, since the fiber used is of more than few meters (100 meters) and since the inner cladding region has lower refractive index than the inner or outer core, it is not possible that this cladding region transmit light for such a long distance.

A plausible reason for the extra peak appearing is the combination of light being launched directly from the source into the outer core (graded index multi mode region) and mode mixing of the light in this region. This includes possibility of light getting guided into 2 regions in this outer core separately.

The time delay between Peak 1 and Peak 3 gives us the location of the bend from the output end of the fiber. Therefore, from Figure 7 we can also see where the bend occurred. A bend closer to the output end would have a shorter delay time between the two peaks.

Figure 8 is a curve showing the relationship of the fraction of light in the inner core to the radius of bend curvature. The fraction of light (f) in the inner core is the ratio of the intensity of light in the inner core after bending to the intensity of light before bending. When the value of parameter f equals to 1 it implies that the fiber is not bent. An f of zero (0) means that there is no light left in the inner core. The intensity of light in the inner core is determined by observing the height of the first peak (Peak 1) from the oscilloscope trace. From this calibration curve, we can observe that a 10% decrease in the magnitude of the light in the inner core (i.e. 90% of the original value) corresponds to a bend radius of 36 mm. A 50% decrease in light corresponds to a bend radius of 7 mm.

The experiment also gave us the range of the fiber loop radius for which we get a distinct output signal. The minimum radius of circular loop that gave maximum leakage of light from the inner core to outer core without breaking was 5.5 mm. The maximum loop radius above which we did not observe any change in the inner core signal was 70 mm.

2.4.2 Prototype Development

In our earlier experiments with the optical fiber, the fiber was bent manually and the corresponding oscilloscope signals were recorded. However, in the implementation of the fiber in a WIM system, we need a load transmitting device to bend the fiber when a vehicular load is applied. With this in mind, we designed a prototype load transmitting device which is described in this chapter.

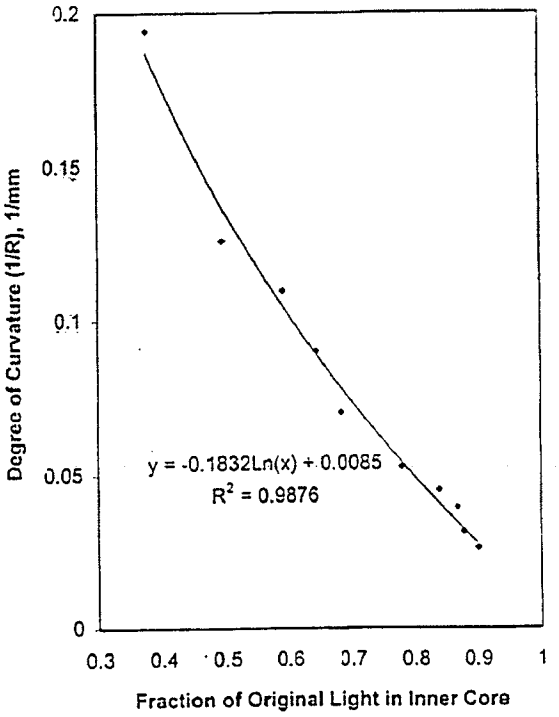

FIGURE 8 Calibration curve Showing Degree of Curvature of Fiber vs Fraction of .Light in Inner Core

2.4.2.1 Proposed WIM Device

Our load transmitting device, shown in Figure 9, is based on a pin and spring mechanism. The device consists of a semi-circular steel top supported by four springs at the four corners on a steel base plate. There are seven pins, three attached to

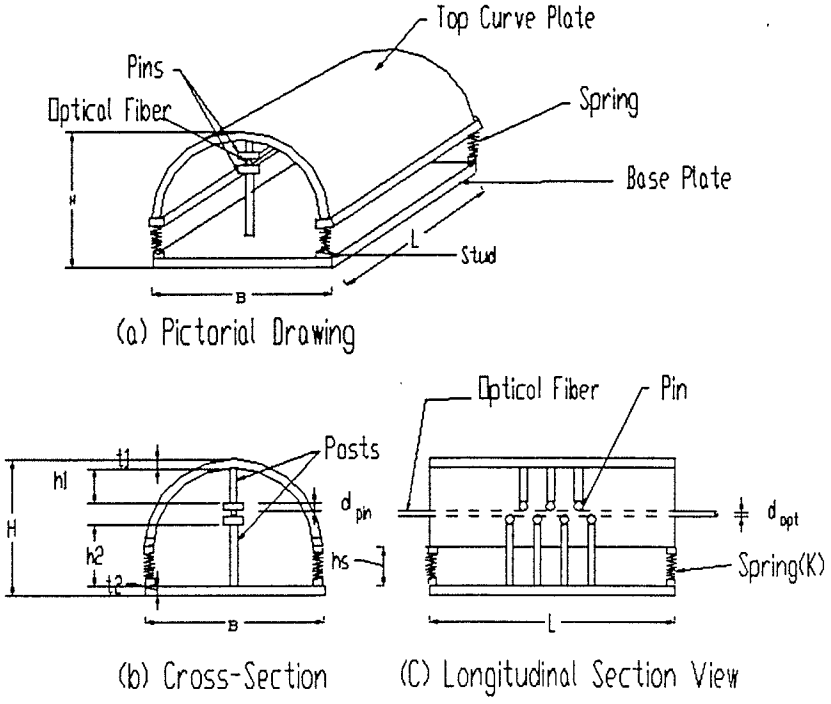

FIGURE 9 WIM Load Transmitting Device

the semi circular top and four attached to the steel plate below. On vehicle wheel loading, the springs would compress causing the pins to push down on the fiber. After the vehicle has passed, the springs would return to their original position. The WIM device is designed to be placed underground with the top just above the road surface. To prevent it from being removed by snow plowing machines and to make it easier for vehicles to pass over it, the device is curved at the top. The individual components of the device are described in detail below.

2.4.2.2 Design of Top Curved Plate

Our aim in designing the top curved plate was to insure that vehicles would be able to go over the device without damaging or overstressing the plate. With this aim, we determined the length, width and safe thickness of the plate.

The length of the device would be equal to a car tire width. The tire contact area for most car tires have a width of approximately 7 in Ref. 29, therefore we designed the length (L) of the device as 8 in. A semi-circular plate of 4 in outer diameter was selected. Therefore, the total width (W) of the device is 4 in.

A structural analysis was performed to ensure that the device would not fail under a particular vehicular wheel load. The thickness of the top plate was determined based on this analysis. This plate was treated as a simply supported arch, since the device has a semi-circular top and is supported by springs at the bottom.

The cross-section of our device is shown in Figure 10. In the figure, there is a load, P, acting on the top of the device. This represents the load caused by a vehicle wheel. This load results in reaction forces at the two ends of our device. The reaction forces occur at the springs (P/4 on each spring) which are present at the four corners of the device. These reaction forces are each equal to P/2 since the load is assumed to be at the center of the device. A section of the device with all the forces acting is shown in Figure 11.The bending moment, M, at an arbitrary section AA' in the device, is given by:

$$M = R_1 x \qquad (2)$$

where x is the horizontal distance from the reaction force (R_1) to the section AA' (R_1 equals P/2). V in the diagram is shear force.

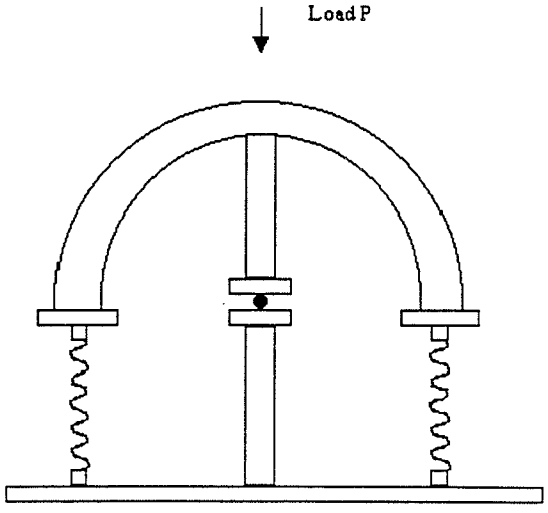

FIGURE 10 Cross Section of Device

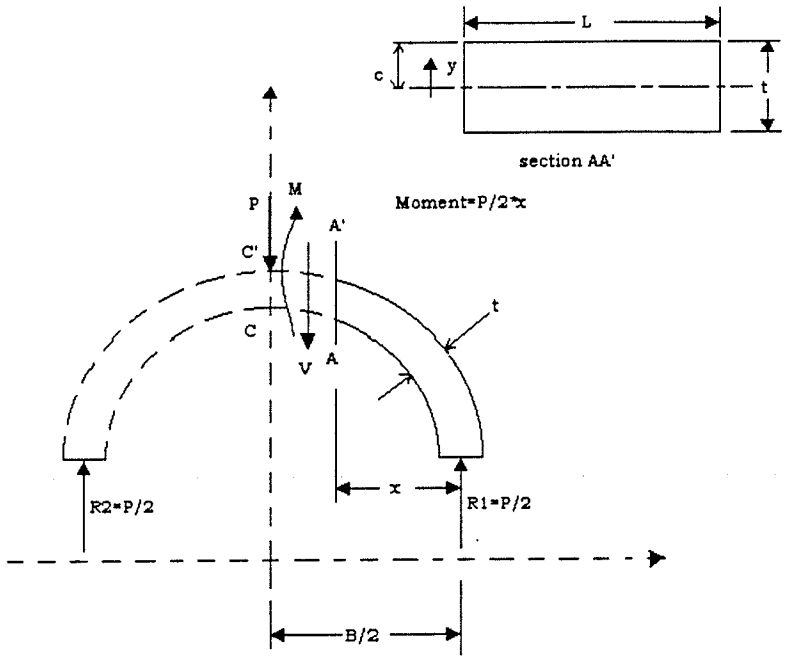

FIGURE 11 Free Body Diagram of Device

Due to this bending moment, the device will undergo stress along AA'. From the basic mechanics of material theory. The relation between the bending moment and the stress within the elastic regime is given in Ref 30:

$$\frac{M}{I} = \frac{\sigma}{y} \tag{3}$$

where,

M = Bending Moment at the Section A-A'
I = Moment of Inertia of the Cross-Section
σ = Stress at any point in the Cross-Section at distance y from the Neutral Axis
y = Distance of the point where stress is measured from the Neutral Axis of the section.

The stress will be maximum at the outermost fiber, where y is the maximum. Since the cross-section at AA' is symmetric about the neutral-axis, the maximum stress will be developed at a distance equal to half the thickness of the device.

From Equation (2) it is seen that the maximum bending moment will occur at the mid-point of the device where the value of x is equal to B/2, B being the width of the device. Thus, the maximum stress occurs along the plate section CC' which is at the mid-point of the device and at a point on the top or bottom outermost fiber. Substituting Equation (2) into Equation (3) with appropriate expressions for x and y, we et the maximum normal stress as:

$$\sigma_{max} = \frac{PBc}{2I} \tag{4}$$

where,

P = Force due to the Load
B = Width of the Device
c = Half Thickness of the Device
I = Moment of Inertia of the Cross Section AA'.

The moment of inertia of a rectangular cross-section at CC' is given by,

$$I = \frac{Lt^3}{12} \tag{5}$$

where L is the length of the device and t is the thickness of the device. With this value of the moment of inertia, and noting c = t/2 Equation (4) gives,

$$\sigma_{max} = \frac{3PB}{t^2 L} \tag{6}$$

Our purpose is to find the required thickness (t) of our device to withstand vehicular wheel loads. Hence the thickness as a function of the other parameters is given by:

$$t = \sqrt{\frac{3PB}{L\sigma_{max}}} \tag{7}$$

The load P is the value of each wheel of a vehicle. For passenger cars the load P is approximately 1000 lbs. There will be an impact factor due to the fact that the vehicle will be in motion and so we set the impact factor as 1.3. The new load is thus 1300 lbs, or 1.3 kips. The width of the device is selected to be 3.625". The length of the device is 8". The value of the yield stress of steel is 36 ksi. We added a factor of safety of 1.5, so the value of the allowable stress, (σ_{max} in Equatiojn 7) is 24 ksi. By substituting these values in Equation (7), we calculated the thickness, t, to be 0.27 inches. This means that with a thickness of 0.27 inches, the maximum stress developed in the top curved plate will be equal to the allowable stress for steel. The curved steel plate that was available to us had a thickness of 0.375" which is more than adequate for our purpose. This was used for our device.

2.4.2.3 Design of Springs

In order to design the springs (i.e. to determine the spring stiffness) for the device, we need to know the maximum vertical displacement of the top pins in the device beyond which the intensity in the output signal would not change. Figure 12 explains the scenario where a pin is pushed down between adjacent pins and the corresponding bending of the fiber is measured. It shows Pin X being pushed down between two surrounding pins, Pin Y and Pin Z. The set of pins shown is a magnified view of the pins in the longitudinal section view of the device (Figure 9c). This figure is also shown here for reference. The bent length of the fiber (ABCD) remains the same as the pin moves down beyond Position 2. Since it is the bending of the fiber that causes the output signal to change, we do not expect to see any change in the output signal when the pin moved beyond Position 2 (i.e. from Position 2 to Position 3 to Position 4). Changes in the output signal are expected only when the bottom of Pin X moves from Position 1 to Position 2. Therefore, if the pins are placed touching each other, the springs should have a total spring constant such that they would depress to a maximum distance equal to one pin diameter under the maximum vehicle wheel load expected.

However, in all practical cases, we would see some gap (horizontal spacing) between two adjacent pins to facilitate fiber insertion. This distance would increase the maximum distance the pin could be depressed before the output signal stopped changing. This horizontal gap between the pins should be kept to a minimum as it would increase the vertical spring displacement and would increase the time the device takes to revert back to its original position after the passage of wheel load.

We chose four springs which would deform the device slightly more than 0.375 inches (diameter of pin used) under the maximum vehicle wheel load considered (1300 lbs). Since most passenger vehicle wheel loads are less than the maximum vehicle wheel load (1300 lbs) considered for design of the design of the device here, these springs would serve our testing purpose. The four springs chosen have a total spring constant of 2720 lbs/in. The undeformed length of each spring is 2.5 in.

2.4.2.4 Design of Pins

Our bending experiment with the fiber, described in previous subsections, gave us the range of bending radii (from 5.5 mm to 70 mm) which would give us a reading on the oscilloscope. We designed the pins such that the fiber would bend around them with a radius within this range. The pins that were finally selected have a diameter of 0.375 in. There are 7 pins in the device, four connected to the bottom plate and three connected to the top. The centers of the pins are 0.813" apart. Individual pins could be removed from the device as needed to get the desired amount of bending.

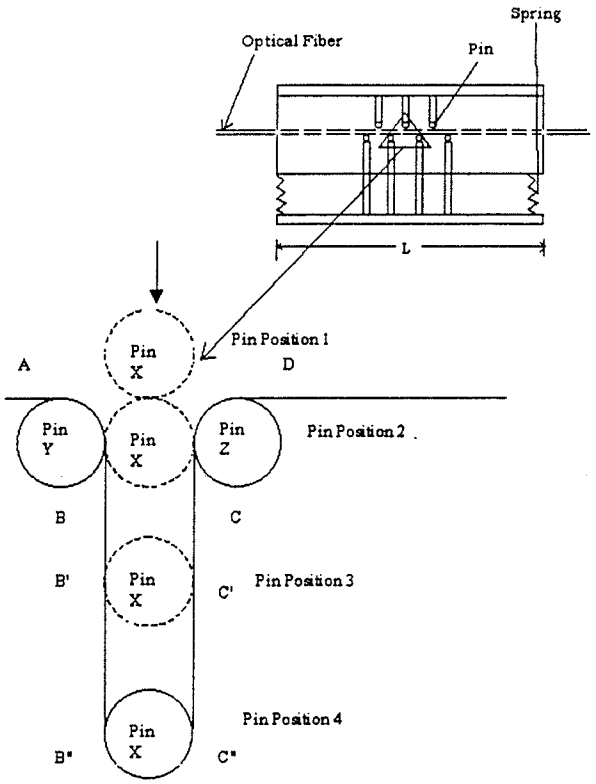

FIGURE 12 Bent Length of fiber

2.4.2.5 Overall Design Details

The base plate of the loading device is 8" long, 6" wide and 7/16" thick. The top curved portion of the device was welded along the length at each of the two edges to two rectangular plates 3/8" thick, 8" in length and 1.5" in width. At the four corners of the base plate, springs were mounted. Four studs are welded to each corner of the base plate and to the two edge plates of the top curved plate above and the springs were fitted on these studs. This arrangement allows easy replacement of springs when needed. The total height of the current device is 5.375" including the thickness of the base plate. Two photographs of the device are shown in Figure 13. The left photograph shows the two halves of the device and the right shows the complete assembly.

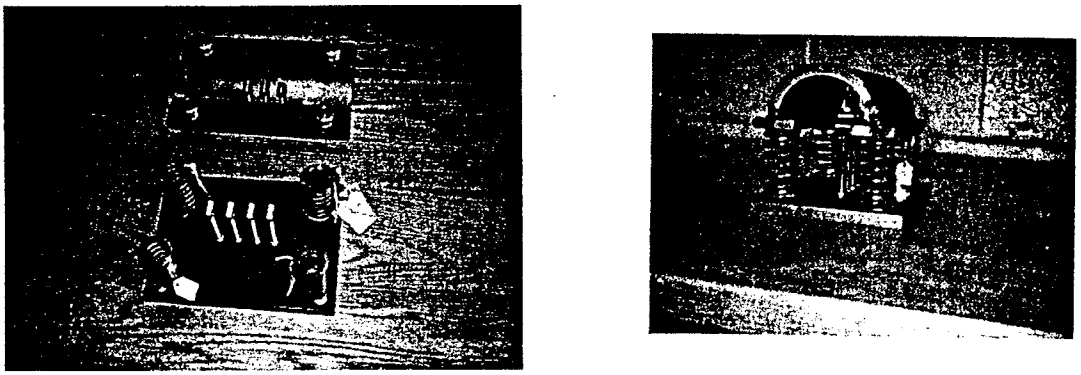

FIGURE 13 Photographs of Loading Device

2.4.3 Prototype Testing

The WIM device was tested in the laboratory under both loading machine and vehicle wheel to evaluate its performance. The first test was done on the SATEC machine. The SATEC machine is a large hydraulic loading device typically used for heavy loads. The second test involved driving a car over the device at a very slow speed.

2.4.3.1 Test under Loading Machine

The WIM device was placed in a SATEC machine and the load was applied in increments of 50 lbs or 100 lbs to a maximum of 850 lbs (Figure 14). The laboratory test had three purposes as listed below:

1. To see whether the device introduced appropriate bending on the fiber to give us the output signal that was expected.
2. To determine the range of loads for which we got a desired output signal. The minimum value of the load that can be measured is that which causes the first noticeable decrease in the inner core light peak intensity. The maximum value of the load that can be measured is that which gives the last noticeable decrease in the inner core light peak intensity. This determines the range of vehicle loads for which the device can be used.
3. To establish a relationship between the applied load and the signal output.

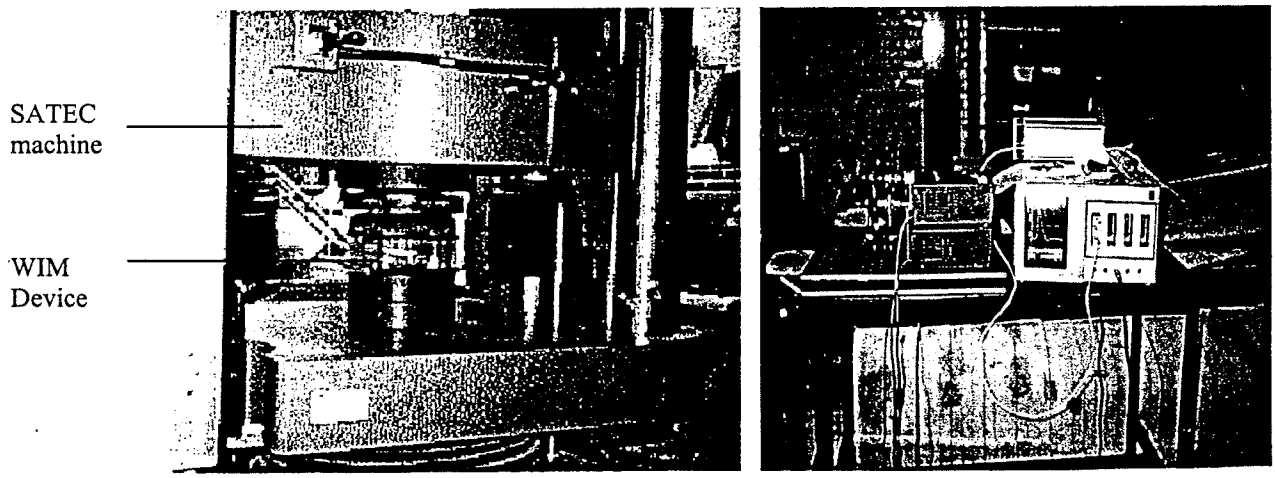

FIGURE 14 WIM Prototype Device Testing Using SATEC Machine

For this load testing, two sets of pin configurations were used in the device. In one, we used a seven pin configuration, four at the bottom and three on top. In the other, we used a three pin configuration, two at the bottom and one on top. In the seven pin configuration, the WIM device was loaded to a maximum value of 350 lb in increments of 50 lb. In the test with the three pin assembly, we loaded the device up to 850 lbs in increments of 100 lb. The maximum load levels were determined based on the inner core and outer core signals. The fiber was 121 feet in length and the WIM device was placed at a distance of 41 feet from the source end.

2.4.3.2 Test Under Vehicle Wheel

This test was performed to see how the device would behave under a vehicle wheel load and whether the test results would be similar to what we obtained from the loading machine test. The test involved a car driving over the device at crawling speed. Future work on the project would involve vehicles driving over the device at higher speeds. The apparatus set-up for the test is described below.

Two parallel wheel tracks each 32 ft long, at vehicle width apart, were built using wooden planks, as shown in Figure. 15. Each wooden plank was 10 inches wide, 5 inches high and 8 feet long. The device was placed in the mid-length of one track.

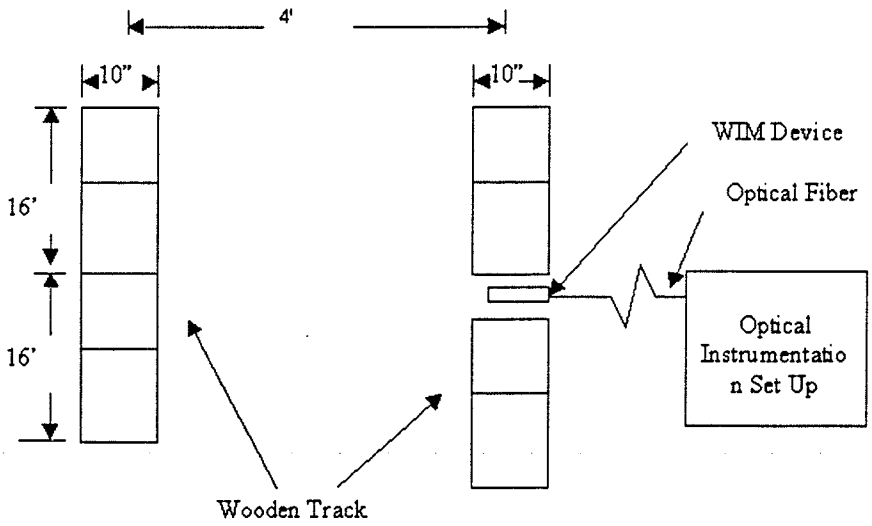

FIGURE 15 Car Test Set Up

There were two tests performed. In the first test we had a fiber of length 121 ft and the loading device was placed 41 ft from the source end. In the second test, we had a fiber of length 71 ft with the device placed 8 ft from the source end. In both tests, the car went over the WIM device at a crawling speed. Two photographs of the car test are shown in Figure 16. The left photograph shows the car track experimental set-up and the right shows the car wheel passing over the loading device.

FIGURE 16 Car Wheel Testing

2.4.4 Test Results

The results from the tests on the prototype WIM device described in Section 2.4.3 are presented here. The data is given in four sections. The first part lists results obtained from the SATEC testing. The second part of this chapter analyzes the results obtained from the 3 pin WIM device testing. This analysis consists of graphs which show the relationship of the three different peaks to the loading. In the third part, the relationship of the output signal to the bent length of the fiber is analyzed. The last part contains data obtained from the car testing.

2.4.4.1 Results from SATEC Machine

The SATEC machine testing was done with the device having 3 pins and 7 pins. Beyond 350 lbs load in the seven pin assembly and beyond 850 lbs in the three pin assembly WIM device, the inner core signal peak was not visible and the signal peak from the outer core was observed to be decreasing. The former observation may indicate that all light from the inner core leaked out of it and the latter indicates that the light began leaking out from the outer core (i.e. out of the fiber).

Therefore, in the seven pin configuration, the WIM device was loaded to a maximum value of 350 lbs in an increment of 50 lbs. In all real life use, the smallest vehicle wheel load is well over 350 lbs, therefore the results from the 7-pin configuration tests are of no practical significance. They have not been reported here.

In the test with the 3-pin assembly, we loaded the device up to 850 lbs in an increment of 100 lbs. The decrease in the number of pins (locations of bending) caused the fiber to have, at each load increment, a total bend length less than that of the 7-pin assembly and therefore we were able to go up to a much higher load in the 3-pin assembly.

Figure 17 shows most of the oscilloscope traces for the three pin assembly. The left peak results because of light going through the inner core, the middle peak results from light being leaked out of the inner core to the outer core at the loading point and the right peak is due to the light entering the outer core at the input end. From the figure, we see that the left peak intensity decreases as the loading increases while the middle peak intensity shows an increase until the loading is 450 lbs beyond which it begins to decrease. This is because beyond 450 lbs load, light begins to leak out of the outer core of the fiber.

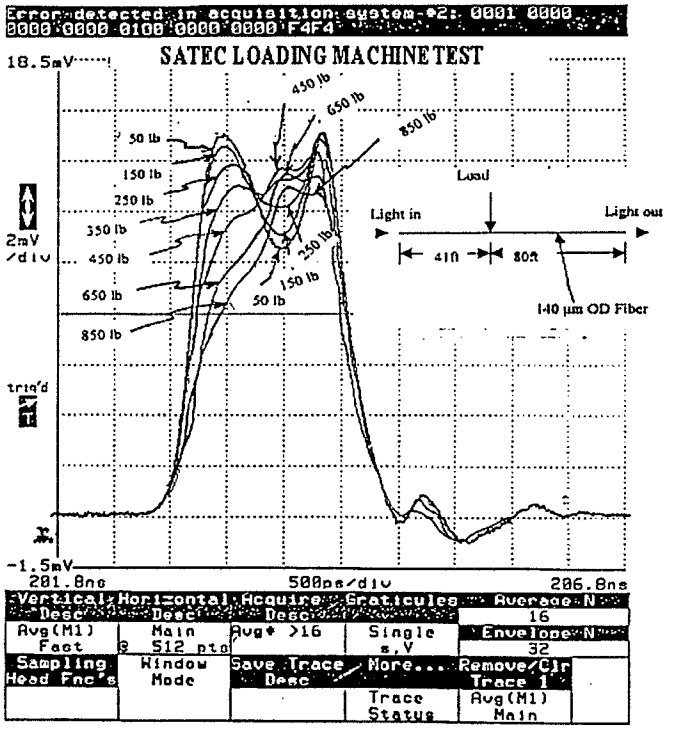

FIGURE 17 Oscilloscope Traces for SATEC Loading Cases for 3-Pin WIM Device

Table 2 gives the loading and unloading results of the SATEC machine test for the 3 pin WIM device. As seen from the table, the left peak intensity decreases with an increase in load. This is expected from theory since the left peak intensity is due to the light in the inner core and will decrease on bending (i.e. loading). The middle peak intensity shows an increase up to a loading of 450 lbs and decreases on additional loading. This decrease may be caused by light escaping from the outer core upon further bending. The last column shows the intensity which results from light being launched unto the outer core at the input end.

TABLE 2 Three-Pin WIM System Loading and Unloading

Load (lb.)	Vertical Displacement (in.)	Left Peak Intensity (mV)	Middle Peak Intensity (mV)	Right Peak Intensity (mV)
50	0.0603	15.5	11	15.6
150	0.144	15.1	11.6	15.75
250	0.182	14.3	12.7	15.5
350	0.2268	13.1	13.7	15.4
450	0.2662	11.9	14.3	15.1
550	0.3057	10.7	14.1	14.5
650	0.3457	10	13.9	13.9
750	0.386	9.3	13.7	13.6
850	0.4255	8.9	13.4	13.2
750	0.3912	9.9	14.1	14.1
650	0.352	11	14.6	14.8
550	0.309	11.9	14.4	15.3
450	0.2675	13.1	13.9	15.4
400	0.2485	13.7	13.5	15.4
350	0.2283	13.9	13	15.4
150	0.1563	15.3	11.1	15.6
50	0.0827	13.5	10.9	15.6

2.4.4.2 Analysis of SATEC Test Results

In order to create a reliable WIM system, we must have a strong relationship between the output signal and the applied load. From the above data, graphs have been plotted showing the relationship of the left and middle peak intensities with the applied load. The graphs have been shown on Figures 18 and 19. We have drawn the graphs for both the loading and unloading cases. Ideally the data points for the two cases, loading and unloading, should match exactly. However, we see that there is a slight difference in the data point values for the two cases. This phenomenon is called hysteresis and will be addressed in future work. The right peak did not show any significant change with loading and therefore the graph for the right peak has not been drawn.

As can be seen from the graphs, the left peak intensity decreases with an increase in the loading. The relationship of the left peak intensity to the applied load is quite strong, (the coefficient of regression value, R being 0.99), and we felt that we should use the left peak readings for our future WIM work. The middle peak, resulting from light in the outer core due to bending, did show an increase on addition of load, but there is not a very strong relationship.

From the oscilloscope traces in Figure 17 we can see that the spatial resolution is pretty good. Our load was at a distance of 80 ft from the output end and for this distance, the left and middle peaks were placed 500 picoseconds apart. Therefore, for vehicles separated from each other by one lane width (12 ft) we would get a separation of about 75 picoseconds. In this way, we would be able to distinguish between vehicles traveling in different lanes.

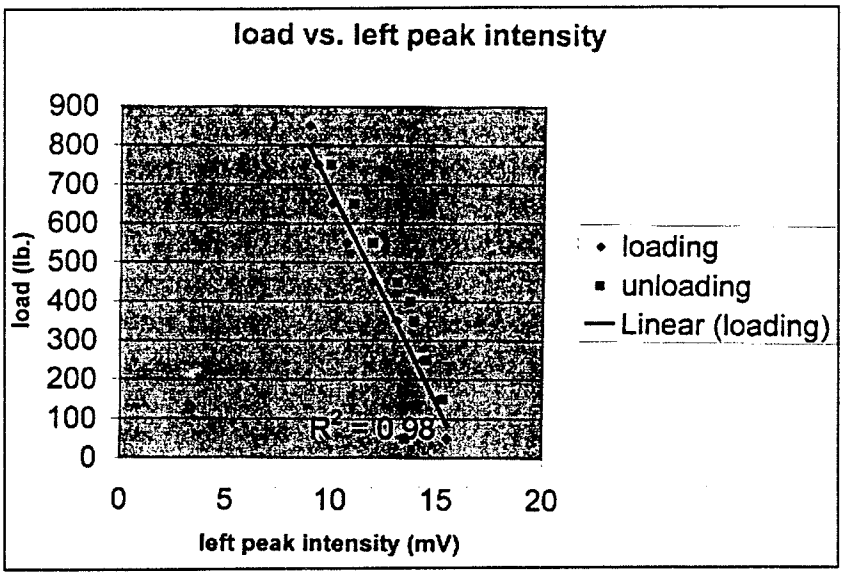

FIGURE 18 Graph of load vs. Left Peak Intensity

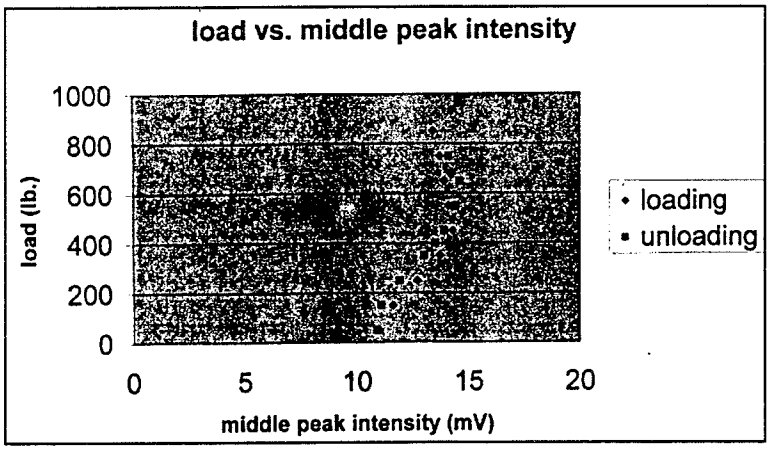

FIGURE 19 Graph of Load vs. Middle Peak Intensity

2.4.4.3 Concept of Bent Length of Fiber

In our experiment, we bent the optical fiber with a series of pins and measured the change in light intensity from the oscilloscope. While it is true that the amount of the vertical deflection that the WIM device undergoes is in direct proportion to the load applied, it is not correct to say that the intensity of light peaks will be in direct proportion to the vertical deflection due to the load. For a given pin diameter and spacing between the pins, the change in the intensity of light is more directly related to the length of the fiber that has been bent. The bent length is in turn related to the vertical displacement of the pin. It is therefore important to determine the relationship between the bend length of the fiber and the output signals because the output signals should have a stronger relationship with the bent length. The details of the mathematical derivation of the bent length of the fiber for a three pin assembly (Figure 20) relating to the vertical displacement of the pin and its diameter is given in Ref 31.

The total bent length around the pins is given by the following expression

$$K = 4R\left(\pi - Cos^{-1}\left(Tan^{-1}\frac{D}{H} - Cos^{-1}\frac{2R}{\sqrt{H^2 + D^2}}\right)\right) \tag{8}$$

where,
K = Total bent length of fiber
R = pin radius
D = center-to-center spacing between the center and adjacent pin
H = vertical depression of center pin

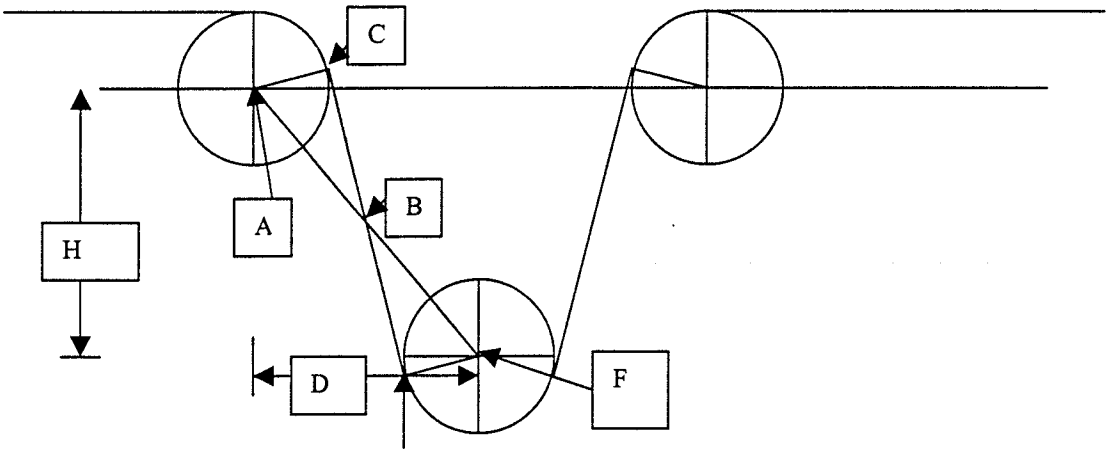

FIGURE 20. Schematic for Fiber Bent Length Determination

Table 3 shows the relationship of the left peak intensity and the bent length. The graph of bent length vs. left peak intensity is shown after the table in Figure 21. As can be seen from the graph, there is a strong relationship of the left peak intensity and the bent length. However, the degree of relationship between the bent length and the left peak intensity is as about the same as that between the vertical displacement and the left peak intensity.

TABLE 3 Light Peak Intensity as a Function of Bent Length

Load (lbs.)	Bent Length (in.)	Left Peak Intensity (mV)	Vertical Displacement of Upper Pin (in.)
50	0.052	15.5	0.0603
150	0.118	15.1	0.144
250	0.15	14.3	0.182
350	0.187	13.1	0.2268
450	0.22	11.9	0.2662
550	0.252	10.7	0.3057
650	0.285	10	0.3457
750	0.318	9.3	0.386
850	0.35	8.9	0.4255
750	0.322	9.9	0.3912
650	0.29	11	0.352
550	0.255	11.9	0.309
350	0.188	13.9	0.2283
250	0.160	14.5	0.1935
150	0.128	15.3	0.1563
50	0.067	13.5	0.0827

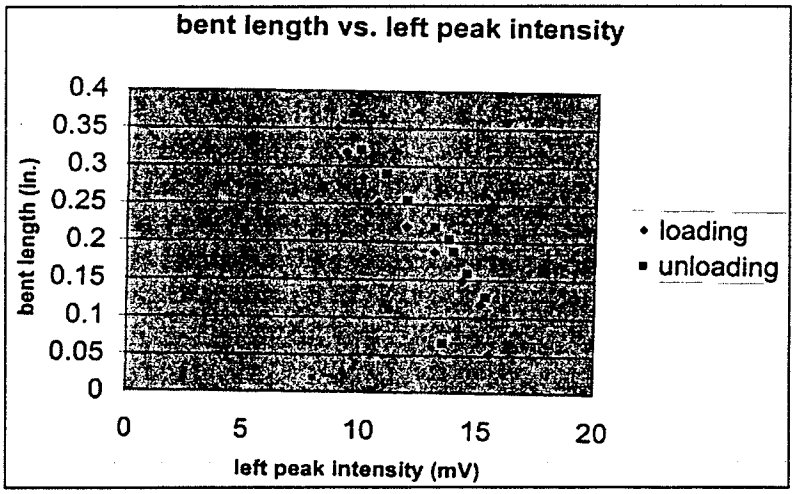

FIGURE 21 Graph of Bent Length vs. Left Peak Intensity

2.4.4.4 Car Test Data

The car test was performed to see whether the system showed the same results under a car wheel load as it did under the static loading machine test. The speed of the car was very slow, about 5 mph. The oscilloscope traces from the car test are shown in Figure 22. The output signals were very similar to what we obtained with the loading machine tests.

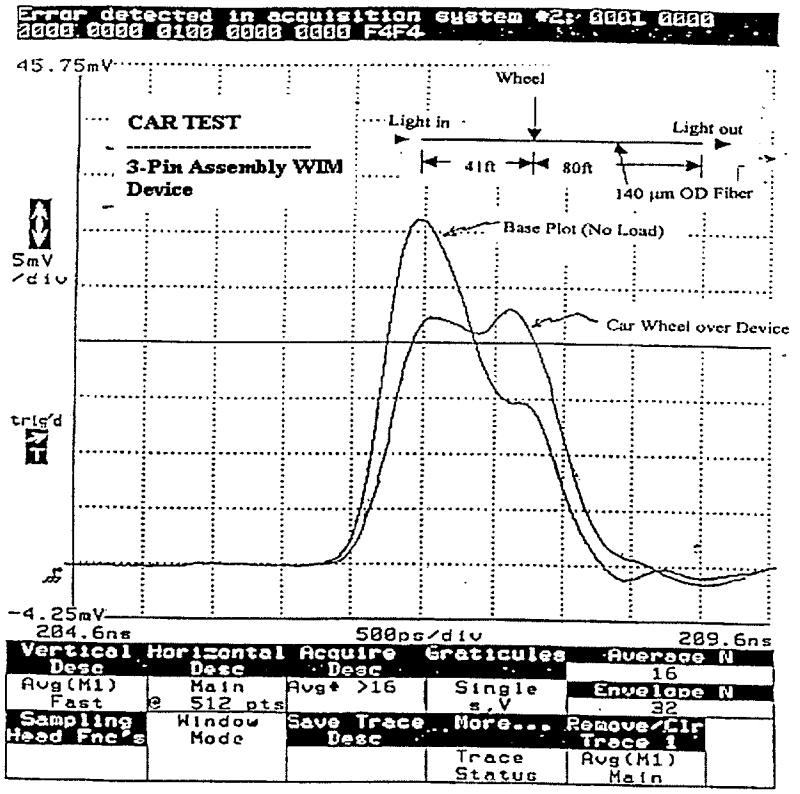

FIGURE 22 Car Test Oscilloscope Traces

Due to the low speed the moving weight of the car was very close to its static weight. One of the main problems associated with WIM research has been obtaining static weight from dynamic weight. This problem has not been addressed in this work. More experiments need to be performed with vehicles moving at higher speeds to get this data.

The spatial resolution from the test was quite good; as in Figure 22, the difference between the two peaks was about 500 picoseconds for the load applied at a point approximately 80 ft from the output end.

2.4.5 Computer Data Acquisition

In order to make the WIM system applicable to real life applications, the data acquisition system needs to be automated. Our data acquisition involved three essential components (Figure 23). A Tektronix oscilloscope (model # 7854) with sampling head (Model # S4) and Time base (model # 7T11A), a Pentium 166 computer operating Windows 95 and Lab View software version 5.0 for Windows 95 from National Instruments.

To store the automatic readings from the oscilloscope directly into a personal computer, we installed a General Purpose Interface Bus (GPIB) card in the computer to interface with the oscilloscope. The card was made by National Instruments (Model # GPIB-PCIIA) and runs on IEEE standard 488.2 protocol *(32)*. After the card was installed, a GPIB cable was used to connect the computer and the oscilloscope.

Lab View utilized the card as an interface to communicate with the oscilloscope. We then programmed it to simulate the functions of the oscilloscope and executed a series of commands from the computer (Figure 24). Those commands functioned exactly like the buttons on the front panel of the oscilloscope. The simulation of an instrument also is called as a Virtual Instrument.

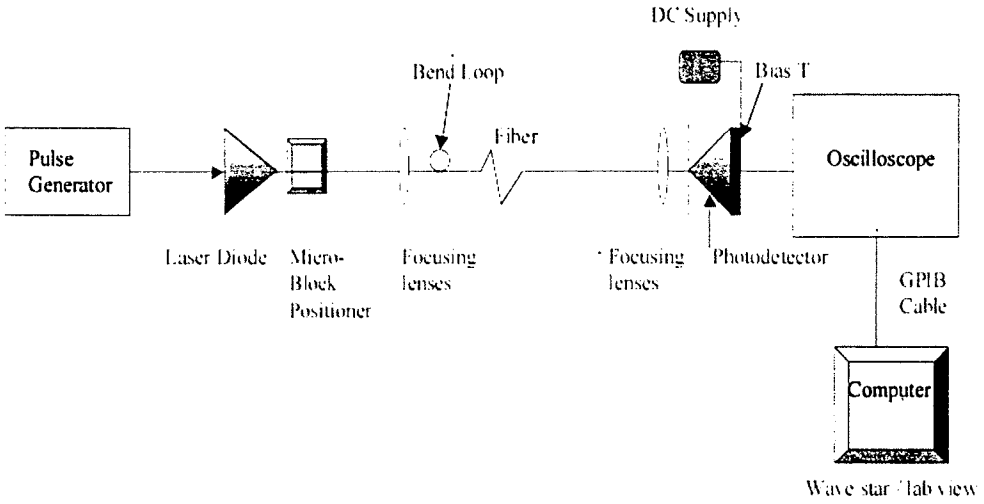

FIGURE 23 Optical Experimented Setup

The whole data acquisition procedure/functions are outlined below:

1. Computer gives commands to the oscilloscope.
2. Oscilloscope acknowledges and executes it.
   i. Oscilloscope freezes the trace and captures it.
   ii. The trace is then transformed to 512 consecutive point data and stored temporally in the memory of the oscilloscope.
   iii. A "find maximum" command finds the global maximum points among the 512 data points.
3. Both the waveform data and maximum value are transmitted back to personal computer and stored as an Excel file.
4. Trace data are plotted on the computer screen which correspond to the trace displayed on the oscilloscope.
5. Computer plots are saved as a Graphic Image File (GIF) file.

Figure 24 shows the graphical interface front panel designed for the oscilloscope and Figure 25 shows the main part of the graphical block diagram program.

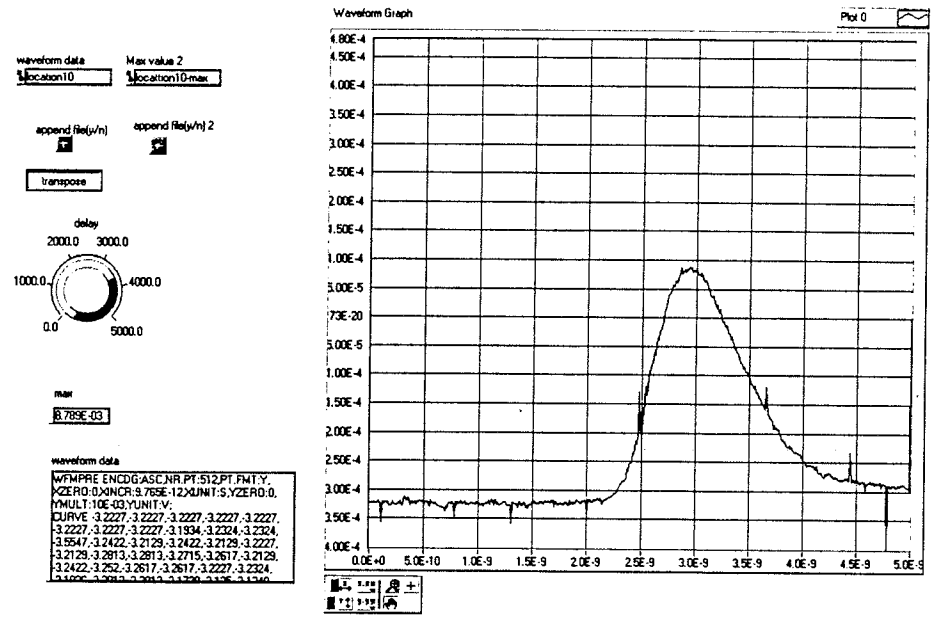

FIGURE 24 Lab View Front panel

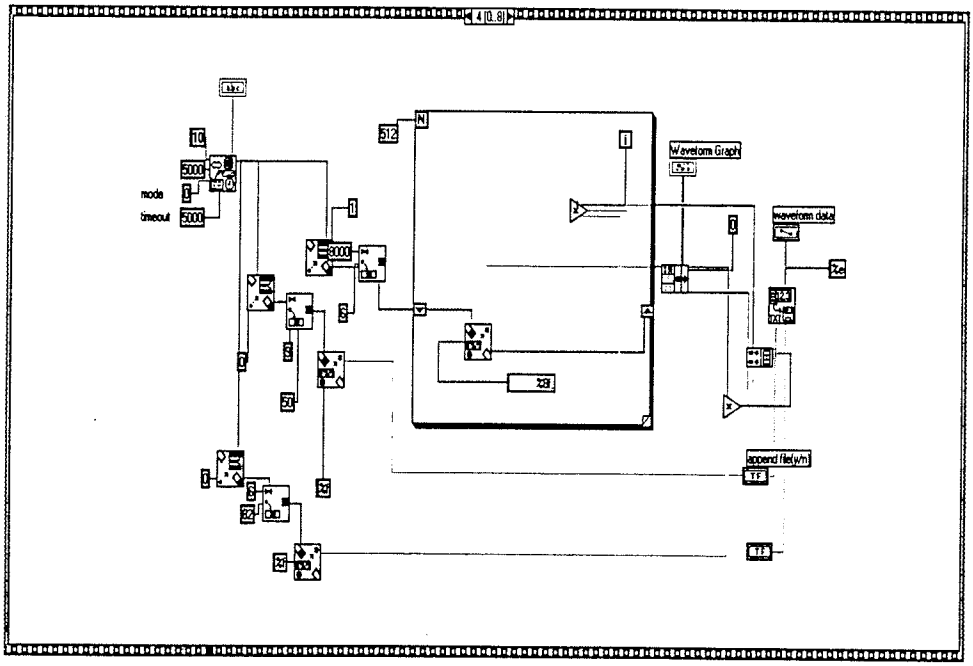

FIGURE 25 Lab View Block Diagram

The primary control shown on the front panel of Figure 25 includes:

- Two text windows where users are required to input two file names to save the data for the waveform and maximum value among all the sampled points.
- Three Boolean buttons for changing the status of the file storage format; etc. transposed (Y/N).
- Two data windows used to display the transmitting data. One is for waveform data and the other for max value as describe before.
- A knob to control the time interval for each data acquisition.
- Waveform plot, where the vertical is volts and horizontal is time in second.

There are several benefits of using a Virtual Instrument:

1. Accuracy. The data can be resolved up to four decimals. When compared to that read from the trace plot, it provided better precision upto 2 significant digits more.
2. Efficiency. We can just set the computer to repetitively collect data at every time interval without having to keep pressing buttons to get readings
3. Convenience. The data are stored in Excel format and ready for further analysis.
4. Accessibility. Both waveform plot and data files can easily be access for modification and comparison.

However, there is still limitation for the data acquisition process. It takes at least 3 seconds to acquire a set of data. This time lost is mostly due to the internal process of the oscilloscope and data transmitting from the oscilloscope to the computer through GPIB cable. This means, when two load applications come on the WIM device within 3 seconds, there would be a potential problem. This computer automated data collection process was not implemented to collect data presented in this report. However, in the future, we intend to verify the system accuracy for data collection

2.5 PLANS FOR IMPLEMENTATION

The Connecticut Department of Transportation (CTDOT) has been involved with the project form its conception. In this phase of study one member from CTDOT has served on the project advisory panel. It is anticipated that they will provide help and advice for the field-testing. We also anticipate that they will serve as beta testers for the prototype. The advisory panel consists of members with connection to user agencies (including FHWA) and industry. The advice of this panel continues to be valuable in product development and technology transfer. The Connecticut Department of Motor Vehicles has also shown interest in the possible product from this project.

To date three Masters level graduate students have received training under this project. Results from the project have been presented at five separate seminars, workshops and conferences (including the NSF/FHWA International Workshop on Fiber Optic Sensors for Construction, Materials and Bridges in May, 1998; Ref. *33)* and have appeared in one publication.

CHAPTER 3.0
CONCLUSIONS AND RECOMMENDATIONS

This section presents conclusions and recommendation for future work. The ultimate goal of this project, of which this is the initial phase(NCHRP - IDEA Type 1: concept feasibility study), was to develop an accurate, reliable and user-friendly weigh-in-motion (WIM) system. This phase of the project began in June 1997 and expired August 1999.

3.1 CONCLUSIONS

The first task was to characterize the fiber. A bending experiment was performed on the fiber to evaluate the theoretical principle of movement of light through the different regions of the fiber.

The second task was designing and fabricating a prototype fiber-optic WIM system. Our third task was to perform bench scale tests to verify the system performance. The system was tested both with a static loading machine and with an actual vehicle. In the vehicle test, the prototype WIM was installed between wooden tracks. The vehicle (a passenger car) was then driven over the system while the optical signal was recorded for various locations of the car as it traversed the prototype WIM.

The laboratory test results of the prototype WIM proved to be very promising. The WIM sensing device showed a very good relationship between the load and the changes in the optical signal. In addition, we were able to pinpoint the location of load application to a fair degree of accuracy. Furthermore, the changes in the optical signal during testing with the car were quite similar to that obtained for the load machine. Based on these results we believe that our prototype device shows a great potential for accurately determining the magnitude and location of vehicle loads.

3.2 RECOMMENDATIONS FOR FUTURE WORK

The future work of the project should include feedback in improving the optical fiber fabrication, improving the current prototype device and conducting field testing. To get better performance from the fiber, there is need for adjustment in refractive indices of various regions of the fiber cross section. Especially the outer core graded multimode region needs to be improved to obtain signal as desired. Fabrication of new batch of the special fiber with improved performance will be required. Other major area of improvement needed is in the launching of light from the laser diode to the single mode central core of the fiber and collecting the light from the output end of the fiber to the photo-detector and the signal to the oscilloscope. This involves a very careful and tedious alignment process. For field tests, rugged connector systems need to be used between the light source and the fiber input end, and between the fiber output end and the photo detector.

Another area of improvement identified from our testing is the need for a better method for holding the fiber in the system in such a way that it completely reverts to its original position after each load application. This may be achieved by attaching springs in the device so that it reverts back to its original position. We also need to optimize the size of the various components of the WIM system (e.g. width of device, pin size and spacing and spring strength) in order to maximize the signal output. The signal output that we received in the project was very low in intensity and it was difficult to distinguish small changes in loading.

We also need to explore and develop methodology to make the device suitable for multi-lane highways and improve data acquisition. Lastly, more detailed testing with prototype device under vehicle wheel loading is needed. This may include driving trucks at various speeds over the prototype. Finally, the device should be evaluated by deploying it on the road for actual WIM data collection. Work is ongoing considering several of these aspects.

GLOSSARY AND REFERENCES

1. M. S. Mamlouk. Rational Look at Truck Axle Weight. *Transportation Research Record* 1307, TRB, Washington D.C., 1990, pp 8-19.

2. C.E. Lee. Standards for Highway Weigh-In-Motion (WIM) Systems. *ASTM Standardization News,* Feb. 1991, pp 32-37.

3. J.D. Muhs, J.K. Jordan, M.B. Scudiere and K.W. Tobin Jr. Results of a Portable Fiber-Optic Weigh-In-Motion System. *Fiber Optic and Laser Sensors IX, SPIE Proc.1584,* (R.P. DePaula and E.Udd, eds.), 1991, pp 374-386.

4. O. Norman, and R. Hopkins. *Weighing Vehicles in Motion, Highway Research Board. Bull. 50,* Washington D.C. 1952.

5. S.C. Sharma, G. Stamatinos and J. Wyatt. Evaluation of IRD-WIM-5000-a Canadian weigh-in-motion system. *Canadian Journal of Civil Engineering,* Volume 17, 1990, pp 514-520.

6. W. Coffinbargar. Design Criteria for Application of Low Speed Weigh-In-Motion. *ITE Journal,* Vol. 60, No. 10, Institute of Transportation Engineers, Washington D.C., 1990, pp 17-20.

7. W.D. Cunagin, S. Majdi and H. Yeom. Intelligent Weigh-In-Motion Systems. *Transportation Research Record* 1311, TRB, Washington D.C., 1991, pp 88-91.

8. B. Haines, T. TenEyck and A. Pietropola. Pennsylvania Department of Transportation's Weigh-In-Motion Program. *Transportation Research Record* 1311, TRB, Washington D.C., 1991, pp 60-69.

9. D.L. Huft, The South Dakota Bridge Weigh-In-Motion System. *Transportation Research Record* 1060, TRB, NRC, Washington D.C., 1986, pp 111-120.

10. B. Jacob, C. Maeder, L. George. and M. Gaillac. *Results of Weigh-In-Motion Project in France.* Transportation Research Record 1410, TRB, Washington D.C., 1993, pp 115-122.

11. C. Koniditsoitis. The Golden River Capacitive Pad Weigh-In-Motion System-Its Life and Times. *Australian Road Research Board,* Victoria, Australia Vol. 15, No. 6, 1990, pp 171-188.

12. C.E. Lee. *A Portable Electronic Scale for Weighing Vehicles in Motion.* Highway Research Record 127: Line Haul Trcuking Costs and Weighing Vehicles in Motion, Highway Research Board, NRC, Washington D.C., 1966, pp 22-33.

13. *Standard Specification for Highway Weigh-In-Motion (WIM) Systems with User Requirements and Test Method.* Designation:E 1318-90, Annual Book of ASTM Standards, Vol. 04.03, 1990.

14. J. J. Trott and J. W. Grainger. *Design of a Dynamic Weighbridge for Recording Vehicle Wheel Loads.* RRL Report LR 219, Road Research Laboratory, Crawthorne, Berkshire, 1968.

15. J. J. Hajek, J. Billing, P. Hoang and A. J. Ugge. *Use of Weigh-In-Motion Scale Data for Safety-Related Traffic Analysis.* TRR 1467, Traffic and Roadway Accident Analysis and Traffic Records Research, 1994, pp 38-43.

16. *Weigh-In-Motion (WIM) Standard to Assist in Collecting Traffic Data.* ASTM Standard. News, July 1990, pp 27-28.

17. R. J. Heywood and C. O'Conner. A Bridge Design and Evaluation Method Derived From Weigh-In-Motion Data. *Canadian Journal Of Civil Engineering,* Vol. 19, No. 3, 1992, pp 423-431.

18. B. Taylor and R. Klashinsky. New Application for Weigh-In-Motion Technology. *Traffic Technology International,* UK & International Press, Surrey, England, 1995, pp 220-225.

19. J. H. Wyman. An Evaluation of Currently Available WIM Systems. *Proceedings of Third National Conference on Weigh-In-Motion*, March 1989, pp 6-176.

20. A.T. Papagiannakis, W.A. Phang, J.H.F. Woodrooffe, A.T. Bergan and R.C.G. Haas. Accuracy of Weigh-in-Motion Scales and Piezoelectric Cables *Transportation Research Record 1215*, TRB, Washington D.C., 1988, pp 189-196.

21. B. Cottrell, Jr. Evaluation of Weigh-In-Motion Systems *Final Report. FHWA Report FHWA/VA-92-RB*, VTRC 92-RB, Nat. Tech. Info. Service, Springfield VA, 1992, 100p.

22. M. Gloverand and W. Newton. Evaluation of a Multi-Sensor Weigh-In-Motion System. RR 307 *Transport and Road Research Lab.*, Crawthorne, England 1991.

23. A.M. McDonnell. Bringing Piezoelectric Weigh-In-Motion On-Line At LTPP Sites In Connecticut. *The National Traffic Data Acquisition Conference*, Sep. 21, 1994.

24. J. Boby, S. Teral, J.M. Caussignac and M. Siffert. Weighing of Vehicles in Motion Using Fiber Optic Sensors. *Electrical Communication 1st Quarter*, 1994, pp 74-77.

25. A. Safaai-Jazi, S.A. Ardekani and M. Mehdikhani. A Low-Cost Fiber Optic Weigh-In-Motion Sensor. *SHRP-IDEA/UFR-90-002,SHRP-89-ID03*, Strategic Highway Research Program, NRC, TRB, Washington D.C., 1990, 62p.

26. K.W. Tobins Jr. and J.D. Muhs. Algorithm for a Novel fiber-optic weigh-in-motion sensor system. *SPIE Proceedings*, Vol. 1589: Specialty Fiber Optic Systems for Mobile Platforms, 1991, pp 102-109.

27. A. Stevens, J.R. Spindlow and G.R. Jones, Fiber-Optic Axle Sensors for Vehicle Data Collection. *IEE Conference Publication 320*, IEE, Michael Foraday House, England 1990, pp 148-152.

28. M. Kleinerman and P. W. Kelleher. A Distributed Force-Sensing Optical Fiber Using Forward Time Division Multiplexing. *SPIE, Distributed and Multiplexing Fiber Optic Sensors*, Vol. 1586, 1991, pp 67-77.

29. H. Y. Huang. *Pavement Analysis and Design.* Prentice Hall College Div., November 1992.

30. F. P. Beer and E. R. Johnston Jr. *Mechanics of Materials.* 2nd Ed., Mc Graw-Hill, New York 1992

31. A. Sen. *Weigh-in-Motion usiing a special forward time division multiplexing fiber optic.* M.S. Thesis, Department of Civil and Environmental Engineering, University of Connecticut, Storrs, CT, August 1999.

32. National Instruments Lab View Version 5.0, Manual 1999.

33. R. Malla, N. Garrick, A. Sen and P. Dua. A dual Core Forward Time Division Multiplexing Optical Fiber for Weigh in Motion System. *Fiber Optic Sensors for Construction Materials and Bridges,* Techomic Publishing Co., Lancaster, PA, May pp 251-262